ISSN1027-5495. Functional Materials, 31, No.4 (2024), p. 501-507
doi:http://dx.doi.org/10.15407/fm31.04.501

Synthesis, morphology and optical properties of the luminescent phosphate-molybdate glasses of the P_2O_5-MoO_3-Bi_2O_3-K_2O-$EuPO_4$ system

K. Terebilenko[1], A. Voinalovych[1], V. Borysiuk[1], V. Chornii[1,2], V. Boyko[2], Ya. Zhydachevskyy[3], V. Sheludko[4], S.G. Nedilko[1]

[1]Taras Shevchenko National University of Kyiv, 01601, Volodymyrska st. 60, Kyiv, Ukraine
[2]National University of Life and Environmental Sciences of Ukraine, 03041, Heroiv Oborony st. 15, Kyiv, Ukraine
[3]Institute of Physics, Polish Academy of Sciences, PL02-668, aleja Lotników 32/46, Warsaw, Poland
[4]Oleksandr Dovzhenko Hlukhiv National Pedagogical University, 41401, Kyivska st. 24, Hlukhiv, Ukraine.

Received September 7, 2024

The study deals with synthesis, structure and optical properties of the phosphate glasses of the composition (1-x) *(44.37P_2O_5 - 8.32MoO_3 -2.94Bi_2O_3 - 44.37K_2O) - x$EuPO_4$ (where x = 0, 0.5, 1.0, 2.0, and 5.0 mol. %). The structure, morphology, and optical properties of the glasses have been observed and analyzed with the use of the XRD, SEM, light diffuse reflection, and luminescent methods. It was found that the glasses doped with $EuPO_4$ crystalline particles reveal intensive photoluminescence mainly caused by the $^5D_0 \rightarrow {}^7F_J$ (J = 1 – 4) radiation transitions in the Eu^{3+} ions. Molybdenum (VI) and bismuth (III) oxides modify a vitreous network and can provide wide light absorption bands in the spectral range ~300 – 430 nm and low intensity luminescence bands in the range 300 – 525 nm, too. Based on a comparison of the spectral characteristics of the radiation of Eu^{3+} ions luminescence in $EuPO_4$ crystals and manufactured glasses, it was assumed that the initial $EuPO_4$ particles do not dissolve completely under melting and are present in the manufactured glasses as nanoparticles of small (several nanometers) size. The obtained results indicates that the glasses under study can be used for elaboration of "warm light" emitting devices.

Синтез, морфологія та оптичні властивості люмінесцентних фосфато-молібдатних стекол системи P_2O_5-MoO_3-Bi_2O_3-K_2O-$EuPO_4$. *К. Теребіленко, А. Войналович, В. Борисюк, В. Чорній, В. Бойко, Я. Жидачевський, В. Шелудько, С.Г. Неділько*

В роботі описано синтез, структуру та оптичні властивості фосфатного скла складу (1-x) *(44,37P_2O_5 - 8,32MoO_3 -2,94Bi_2O_3 - 44,37K_2O) - x$EuPO_4$ (де x = 0, 0,5, 1,0, 2,0 і 5,0 мол. %). Структуру, морфологію та оптичні властивості стекол спостерігали та аналізували за допомогою РФА, СЕМ, дифузного відбиття світла та люмінесцентних методів. З'ясовано, що стекла, леговані кристалічними частинками $EuPO_4$, виявляють інтенсивну фотолюмінесценцію, зумовлену, в основному, випромінювальними переходами $^5D_0 \rightarrow {}^7F_J$ (J = 1 – 4) в іонах Eu^{3+}. Оксиди молібдену (VI) і вісмуту (III) модифікують мережу склоподібного тіла і можуть відповідати за широкі смуги поглинання світла в спектральному діапазоні ~300 – 430 нм, а також смуги люмінесценції низької інтенсивності в діапазоні 300 – 525 нм. На основі порівняння спектральних характеристик люмінесценції іонів Eu^{3+}

в кристалах $EuPO_4$ та виготовлених стеклах зроблено припущення, що вихідні частинки $EuPO_4$ не розчиняються повністю при плавленні та присутні у виготовлених зразках скла у вигляді наночастинок малого (кілька нанометрів) розміру. Отримані результати показують можливість використання досліджених стекол для створення приладів, що випромінюють «тепле світло».

1. Introduction

Glasses can be regarded as indispensable materials for numerous applications in a modern technology. In contrast to the polymers, glasses possess much better stability under action of various factors. There is also a possibility for tailoring of some properties of the glasses due to easiness of the variation of their chemical compositions, that cannot be done in case of the crystalline materials. Nowadays, a wide variety of glasses have been used in light emitting diodes [1], optical fibers and fiber lasers [2], sealing technology [3], x-rays shielding material [4], as bioactive glasses [5,6], etc.

According to the Zachariasen's criteria [7] the SiO_2, B_2O_3, P_2O_5, GeO_2, Sb_2O_3, As_2O_3, Ln_2O_3, SnO_2, TiO_3, PbO_2, P_2O_3, Nb_2O_3, Ta_2O_5 can be considered as glass network forming oxides. Among glasses the P_2O_5-based ones are of high interest because of their low toxicity (moreover, high biocompatibility at some compositions), temperature of production (low glass transition temperature, T_g), cheap raw materials, good transparency in a visible spectral range and possibility to achieve high intensity of light emission with introduction of appropriate dopants. In particular, phosphate glasses have been intensively studied for decades as active laser media [8,9]. The main drawback of these glasses is their hygroscopicity that takes place in all the ultra-phosphate (correspond to $2.5 < [O]/[P] < 3$ criteria [10]), and many polyphosphate ($[O]/[P] > 3$) systems. An incorporation of some the network modifiers improves not only stability of the phosphate glasses but also alters other physico-chemical characteristics, in particular, luminescence properties.

This study deals the synthesis, structure, and optical properties of the phosphate glass of P_2O_5-MoO_3-Bi_2O_3-K_2O-$EuPO_4$ composition. In this system molybdenum (VI) and bismuth (III) oxides modify a vitreous network and, additionally, can provide wide light absorption bands in the ultraviolet(UV)/violet spectral regions (~260 – 400 nm). The Bi^{3+} ions and MoO_4^{2-} molecular anions can also reveal luminescence in a wide range from UV up to red region (290 – 800 nm) depending on material [11-16]. The role of K_2O is to maintain [O]/[P] ratio above 3 in order to avoid hygroscopicity of the samples. The $EuPO_4$ was used as a source of Eu^{3+} ions and the latter are known luminescent probes for local surroundings as well as can provide intensive photoluminescence. It was found, that spontaneous crystallization of various bismuth phosphates, primarily $BiPO_4$, may occur in the P_2O_5-MoO_3-Bi_2O_3-K_2O molten system [17]. Such crystallization can be applied for obtaining of optical glass-ceramics with unique physical properties due to interphase formation [18]. However, when crystals became quite large (e.g. tens of microns in size), the light scattering increases at the crystal/glass phase boundary and the material lose its optical quality. Thus, in order to obtain transparent glass or glass-ceramics a spontaneous crystallization should be negligible small or lead to formation of so-called nano-glass ceramics. Such ceramics attracted considerable attention at the last decade as perspective optical materials [19-23].

The goal of the present study was to prepare transparent glasses in P_2O_5-MoO_3-Bi_2O_3-K_2O system with different content of $EuPO_4$ luminescent component by a convenient melt quenching technique. The synthesized samples were characterized by means of X-ray powder diffraction (XRD), scanning electron microscopy (SEM), diffuse reflectance, and photoluminescence (PL) spectroscopy. The peculiarities of the PL properties have been analyzed from viewpoint of transformation of the Eu^{3+} ions nearest surrounding. The color characteristics of the samples were calculated and potential of an application of the prepared glasses in lighting devices has been discussed.

2. Experimental

The polycrystalline $EuPO_4$ was obtained by sol-gel method from Eu_2O_3 (99.9 %, Sigma-Aldrich), and H_3PO_4 (ACS reagent, ≥ 85 wt. % in H_2O, Sigma-Aldrich). The europium oxide was dissolved in orthophosphoric acid to form a colorless solution, and then europium orthophosphate was precipitated using an ammonia solution while controlling the pH of the solution to 7. Subsequently, the precipitate was filtered and dried first at 100 °C for 2 h, then at 400 °C for 6 h, at 700 °C for 6 h, and

at 900 °C for 6 h. The glasses were obtained by quenching technique from (1-x) ($44.37P_2O_5$ - $8.32MoO_3$ -$2.94Bi_2O_3$ - $44.37K_2O$) - x$EuPO_4$ (where x = 0, 0.5, 1.0, 2.0, and 5.0 % mol.) molten system. On the first stage a mixture of MoO_3 (99+%, Thermo Fisher Scientific), Bi_2O_3 (99.9 %, Sigma-Aldrich), KH_2PO_4 (ACS reagent, Sigma-Aldrich), and $EuPO_4$ in a stochiometric amount has been mixed together and placed into platinum crucible. Then the mixture was heated up to 1100 °C and kept at this temperature for 2 hours. Afterward, the melt was poured out on a copper sheet for fast cooling. Here, the glasses are abbreviated as G-xEu, where *x* indicates % mol. of $EuPO_4$ in the system.

X-ray diffraction patterns have been recorded using a Shimadzu XRD-6000 diffractometer with a graphite monochromator in front of the counter (method of 2Θ continuous scanning at a rate of 1 °/min) in the range of 2Θ = 5.0 ÷ 65.0°. Scanning electron microscope Tescan Mira 3 LMU with a 20-nm electronic beam diameter was used for SEM measurements. A Carry 5000 UV-Vis-NIR spectrophotometer with diffuse reflectance accessory (optical integration sphere, DRA-2500) was used to measure diffuse reflection spectra in the range 200 - 850 nm. The photoluminescence and PL excitation spectra were recorded using a Horiba/Jobin-Yvon Fluorolog-3 spectrofluorometer equipped with a 450 W xenon lamp. All the measurements were performed at room temperature. The spectra were corrected on system response.

3. Results and discussion

The XRD patterns (Fig. 1) of the G-0Eu and G-5Eu samples consist of wide bands with maxima near 14, 28.5, 44 and 57° of 2Θ. There are no narrow peaks at the XRD patterns that indicate an absence or at least a low content of crystallite like inclusions. However, the main peaks of the XRD pattern of crystalline $EuPO_4$ (Fig. 1, curve 3) correspond to the indicated bands in the XRD spectra of glass. This observation can be considered as a manifestation of the $EuPO_4$ crystal lattice motifs in the structure of glass.

Typical SEM images of the studied glasses are shown in Fig. 2. There you can see a smooth surface along with a number of particles of chaotic shape and size. The absence of these details in the SEM image taken only in the backscattered electron mode (BSE, right part of Fig. 2) indicates that these particles are located on the surface of the sample and are simply

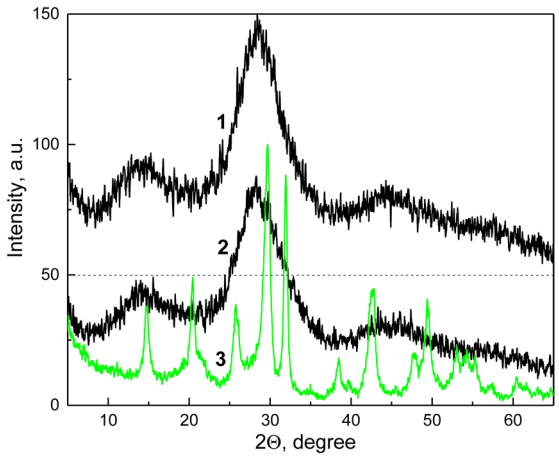

Fig. 1. XRD patterns of the glasses with zero (1) and 5.0 mol. % of $EuPO_4$ (2), and polycrystalline $EuPO_4$ (3). Dashed line depicts "0" signal level for curve 1.

glass chips that settled on its surface during the preparation of the samples for experimental measurements. The crystalline inclusions were not identified in any of the SEM images. Thus, we can conclude that crystalline grains of the $EuPO_4$ powder were undergo melting. Therefore, the residual $EuPO_4$ crystallites are either very small in size (units of nanometers) or the initial $EuPO_4$ concentrations (up to 5 wt. %) were too low to be observed. In addition, we should note that no noticeable self-crystallization occurred during melt quenching.

The diffuse reflection spectra of the G-5Eu glass and $EuPO_4$ powder are shown in Fig. 3, curves 1 and 2, respectively. (It should be noted, that the diffuse reflection spectra of other studied glasses are very similar to those of the G-5Eu glass.) The set of the narrow deeps in the $EuPO_4$ reflection spectrum can be clearly seen at $EuPO_4$ spectrum and none of them can be found at the spectrum of glass. These bands located at 367, 376, 382, 394, 416, 464, 525, 535, and 587 nm should be assigned to the *f* – *f* electronic transitions in Eu^{3+} ions: $^7F_1 \rightarrow {}^5D_4$, $^7F_0 \rightarrow {}^5G_2$, $^7F_1 \rightarrow {}^5L_7$, $^7F_0 \rightarrow {}^5L_6$, $^7F_1 \rightarrow {}^5D_3$, $^7F_0 \rightarrow {}^5D_2$, $^7F_0 \rightarrow {}^5D_1$, $^7F_1 \rightarrow {}^5D_1$, and $^7F_1 \rightarrow {}^5D_0$, respectively [24].

It is also seen that there is a sharp fall in the reflectance with decreasing wavelength. However, if this drop starts at only short-wave lengths ~330 nm for $EuPO_4$ crystals, it starts at ~430 nm for the glass. As for crystals, this related absorption can be ascribed to fundamental absorption edge or, in other words, to electronic transitions from top of the valence band (VB) to bottom of the conduction band (CB) of the material. The smallest energy of such tran-

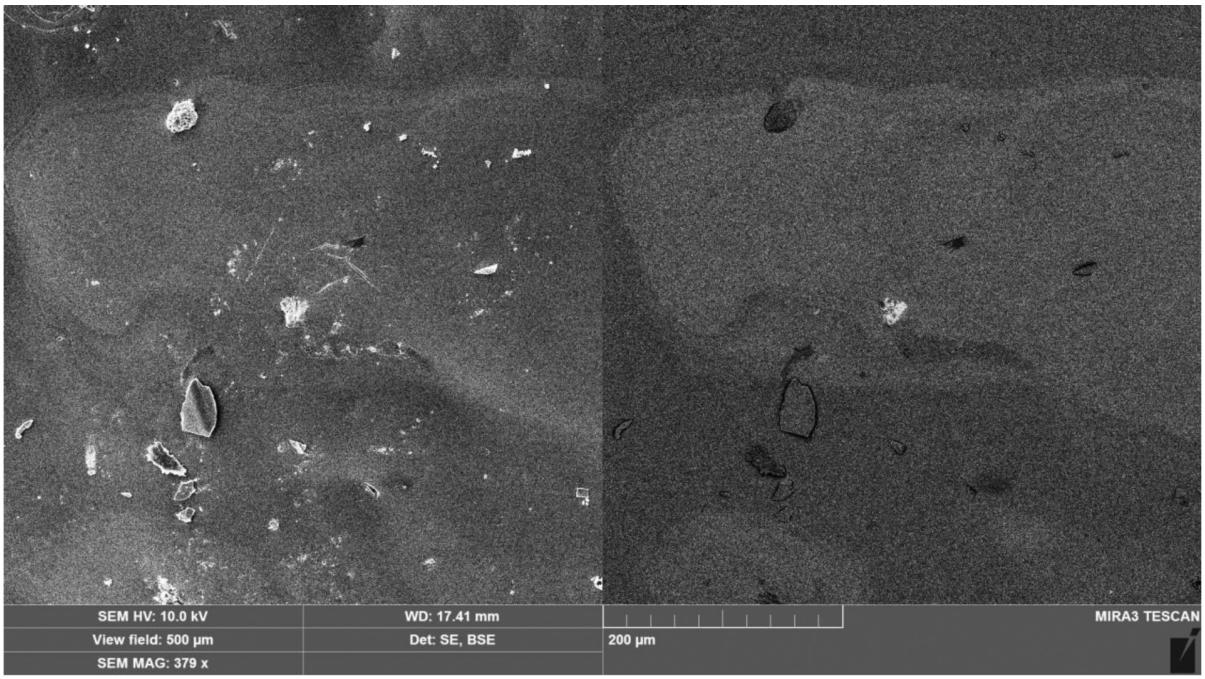

Fig. 2. SEM images of the G-5Eu sample taken at SE-BSE (left) and only BSE regimes (right)

sitions is known as band gap energy, E_g, and it can be estimated from the spectra of diffuse reflection. For this reason, diffuse reflection spectra were converted to absorption spectra by Kubelka-Munk equation [25]. At the next step of the procedure, so called Tauc plots [26] were drawn (see inset in Fig. 3). The estimated values of indirect and direct optical band gaps were evaluated, respectively, by the values 4.18 and 4.55 eV for the $EuPO_4$ crystals, while the corresponding values were estimated as 3.31 and 3.91 eV for the glass. The value 4.55 eV is very close to the E_g value 4.57 reported early in the work [27] for the $EuPO_4$ compound. Both E_g values for glass are much lower. This means that for glasses the additional absorption in the region of $330 < \lambda < 430$ nm is due to components that are not present in the $EuPO_4$ crystals. Obviously, these additional components are bismuth and europium ions located in the oxygen environment.

Taking into account these E_g values, three types of PL excitations were used. First, λ_{ex} = 250 nm (corresponding photon energy $hv_{ex} \approx 4.96$ eV) – it provides excitation due to transition from the top of VB to deep into CB in both $EuPO_4$ and glass. It is possible, that there is a contribution of the charge transfer exciting transition from O^{2-} to Eu^{3+} ions. Second, λ_{ex} = 275 nm ($hv \approx 4.51$ eV) – transition near band edge of $EuPO_4$ and well above of CB bottom in a case of the glass.

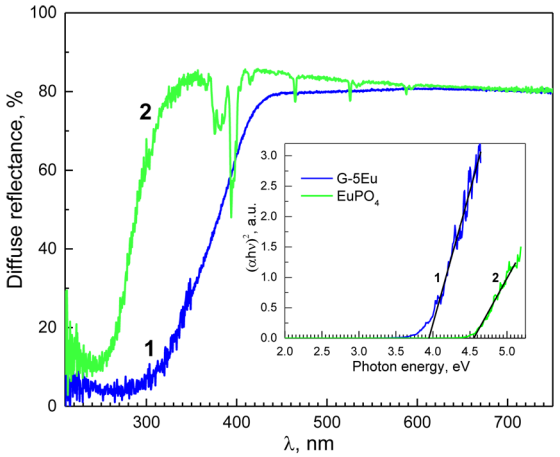

Fig. 3. Diffuse reflectance spectra of G-5Eu glass (1) and $EuPO_4$ powder (2). Inset: Tauc plots corresponding to the curves 1 and 2.

Third, λ_{ex} = 360 nm ($hv \approx 3.44$ eV) – near band edge of glass. The absorption transitions related to defects and/or intrinsic transitions in the electronic *f* - shell in the Eu^{3+} ions can be realized under this excitation.

Excitation spectra of the Eu^{3+}- ions PL are shown in the Fig. 4, curve 1. It is seen, that red emission effectively excited through direct excitation of Eu^{3+} ions. The most intensive excitation lines correspond to the $^7F_0 \rightarrow {}^5L_6$ (λ = 393 nm), $^7F_0 \rightarrow {}^5D_2$ (λ = 464 nm), $^7F_0 \rightarrow {}^5D_1$ (λ = 524 nm), and $^7F_1 \rightarrow {}^5D_1$ (λ = 524 nm) electronic transitions. The "background" at $\lambda < 370$ nm corresponds to excitation of Eu^{3+} ions through the

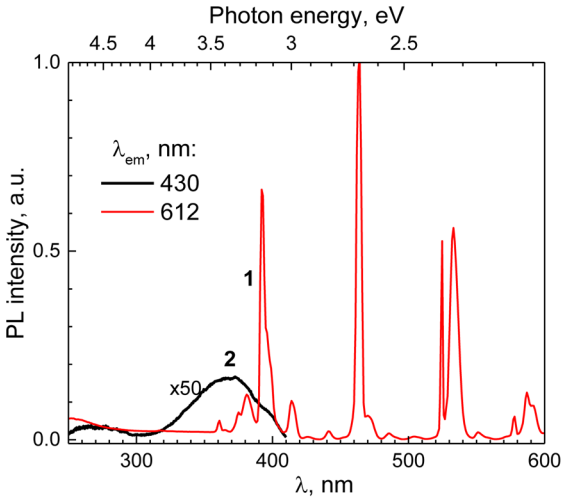

Fig. 4. Excitation spectra of the G-5Eu glass PL registered in the range of Eu^{3+} (1) and host emissions (2).

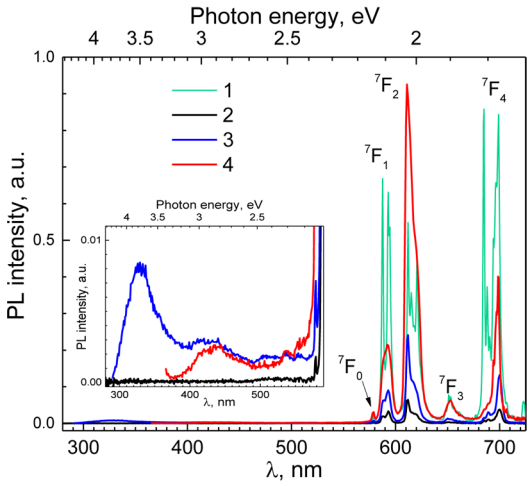

Fig. 5. PL spectra of the $EuPO_4$ (1) and G-5Eu (2 - 4) samples; λ_{ex} = 250 (2), 275 (3), and 360 nm (1, 4).

light absorption of by the glass host ($44.37P_2O_5$ - $8.32MoO_3$ -$2.94Bi_2O_3$ - $44.37K_2O$) with further excitation energy transfer to the Eu^{3+}- ions ($EuPO_4$ - component). The part of the "background" at $\lambda < 270$ nm can be ascribed to $O^{2-} \rightarrow Eu^{3+}$ charge transfer transition in $EuPO_4$.

The corresponding PL spectra are shown in Fig. 5. The PL spectra of $EuPO_4$ at different excitations revealed only the groups of the narrow lines caused by $^5D_0 \rightarrow {}^7F_J$ (J = 0 – 4) electronic transitions in Eu^{3+} ions. The PL spectrum for λ_{ex} = 360 nm is shown in Fig. 5, curve 1. It can be noted that two peaks of $^5D_0 \rightarrow {}^7F_1$ transitions and 5 peaks of $^5D_0 \rightarrow {}^7F_2$ transitions can be found there, that indicates a low symmetry of Eu^{3+} ions position in the crystal structure. This result is in consistence with structural data for hexagonal $EuPO_4$ crystal, where Eu^{3+} cations occupy site positions of C_2 symmetry [28].

The PL spectra of glasses depend on the excitation wavelengths and differ from the PL spectra of the $EuPO_4$ compound. In particular, the $^5D_0 \rightarrow {}^7F_J$ (J = 0 – 4) spectral lines of the Eu^{3+} ion emission in the case of the G:xEu glasses are wider in comparison to the spectra of the crystal. Thus, the fine structures of the $^5D_0 \rightarrow {}^7F_J$ (J = 1 – 4) groups are almost absent for the case of the glasses. This fact is best estimated from the half-width (HW) of the line corresponding to the singlet $^5D_0 \rightarrow {}^7F_0$ transition. It was found that for the case of glass the half-width of this line (76 cm^{-1}) is almost twice as large as for the case of crystal – 45 $см^{-1}$. At the same time, it should be noted that this value is significantly smaller than those typically observed for RE ions in glasses [29].

We can assume that the discussed PL is related to the Eu^{3+} ions which are located in the $EuPO_4$ crystallites, and not in the amorphous medium of the glass. Thus, we suggest that the grains of the crystalline $EuPO_4$ powder are not completely melted during the glass elaboration. Due to the significant reduction in the size of the crystallites, a significant part of the Eu^{3+} ions belonging to them finds themselves in an irregular environment. The consequence of this is a significant inhomogeneous optical broadening, and therefore the half-width of the lines increases. The described phenomenon had been observed earlier for the $EuPO_4$ nanoparticles, in particular in the work [30].

Another observed difference in the PL spectra of glasses, compared to the case of crystalline $EuPO_4$, is the change in the ratio of the intensity of the groups of lines I_1 and (I_2 corresponding to the $^5D_0 \rightarrow {}^7F_1$ and $^5D_0 \rightarrow {}^7F_2$, respectively. It is easy to see that in the spectra of crystals $I_2/I_1 < 1$, while in the case of glass the ratio is inverse, $I_2/I_1 > 1$. The change in the ratio is the result of an increase of the hypersensitive $^5D_0 \rightarrow {}^7F_2$ transition intensity comparing to $^5D_0 \rightarrow {}^7F_1$ transition intensity that indicates lowering of the symmetry of Eu^{3+} ions surrounding. This observation confirms our assumption regarding the irregularity of the Eu^{3+} environment in the samples under study.

Excitation of the Eu^{3+}- related emission at λ_{ex} = 250 and 275 nm is not so effective in comparison with excitation by photons with hv $\approx E_g$ of the glass. However, if excitation is at λ_{ex} = 275 nm three weak bands of intrinsic emission of the glass host near 328, 438, and 518 nm are seen (inset in Fig. 5).

Table 1. Chromaticity coordinates (x, y), correlated color temperature (CCT) and color purity (CP) of the G-5Eu glass emission

λ_{ex}, nm	*x*	*y*	CCT, K	CP, %
250	0.620	0.357	2087	84.69
275	0.608	0.339	2282	82.93
360	0.653	0.340	2898	94.76
393	0.649	0.351	2530	93.80
465	0.660	0.339	3032	97.51

The Fig. 4 shows that the violet intrinsic PL of the host is mainly excited in the 250 – 410 nm range. Taking into account the results of band gap estimation both the PL excitation band can be ascribed to "regular" moieties of glass network – Bi^{3+} ions in oxygen surrounding and MoO_4^{2-} molecular anions. However, at the current stage of the study, it is hard to ascribe the intrinsic emission of the glasses to specific luminescence centers.

Nevertheless, high intensity of Eu^{3+}- related luminescence as well as the high optical quality of the studied glasses suggest their possible application in light-emitting devices.

For this reason, CIE 1931 chromaticity coordinates (*x,y*), correlated color temperature (CCT), and color purity (CP) have been calculated by the methods described in literature [31, 32]. The calculated values of the color characteristics for G-5Eu sample are collected in Table 1. It can be seen that the chromaticity coordinates if the PL was excited at 465 nm, are close to those for the standard of red color (x = 0.64; y = 0.34). High color purity values were obtained for all the used excitation wavelengths. Calculated correlated color temperature (T < 4500 K) indicates that the glasses under study can be used for elaboration of "warm light" emitting devices.

Conclusions

For the first time, glasses of the (1-x) $*(44.37P_2O_5 - 8.32MoO_3 - 2.94Bi_2O_3 - 44.37K_2O) - xEuPO_4$ (where x = 0, 0.5, 1.0, 2.0, and 5.0 % mol.) system were synthesized and their properties have been studied.

Glasses XRD patterns reveal wide bands typical for amorphous glassy materials. There were no narrow crystal-type peaks observed. Thus, XRD data indicate an absence or at least a low content of crystallite-like inclusions in the glass bodies. At the same time, it is important to note that the mentioned bands correspond in position to clusters of the main peaks in the XRD spectra of the $EuPO_4$ crystals.

SEM images showed no noticeable self-crystallization of the made glasses.

Luminescence studies have shown that the photoluminescence of glasses is caused mainly by the emission of Eu^{3+} ions, which can be considered here as luminescent probes of material structure.

Taking into account the difference in the spectral characteristics of the Eu^{3+} - ions emission in the studied glasses and $EuPO_4$ polycrystals (spectral width of lines, intensity distribution in groups of the $^5D_0 \rightarrow {}^7F_J$ (J = 1 – 4) multiplets), an important conclusion was made regarding the location of the Eu^{3+} - ions in the volume and surface of residual $EuPO_4$ nanocrystallites.

The high optical quality, calculated chromaticity coordinates, correlated color temperature, and color purity characteristics have pointed the glasses studied possible application in light-emitting devices.

Acknowledgements

This work has received funding through the EURIZON 3010 project which is funded by the European Union under grant agreement No.871072.

References

1. Y. Hu, Y. Ye, W. Zhang et al., *J. Mater. Sci. Technol*., **150**, 138 (2023).
2. W.C. Wang, B. Zhou, S.H. Xu et al., *Prog. Mater. Sci*. **101**, 90 (2019).
3. A. de Pablos-Martín, S. Rodríguez-López, M.J. Pascual, *Int. J. Appl. Glass Sci.*,**11,** 552 (2020).
4. S. Kaewjaeng, S. Kothan, W. Chaiphaksa et al., *Radiat. Phys. Chem*., **160**, 41 (2019).
5. H.E. Skallevold, D. Rokaya, Z. Khurshid, M.S. Zafar, *Int. J. Mol. Sci.,* **20**, 5960. (2019).
6. Z. Neščáková, K. Zheng, L. Liverani et al., *Bioact. Mater*., **4**, 312 (2019).
7. W.H. Zachariasen, *J. Am. Chem. Soc.* **54**, 3841 (1932).
8. C.G. Young, *Proc. IEEE*, **57**, 1267 (1969).
9. N.G. Boetti, D. Pugliese, E. Ceci-Ginistrelli et al., *Appl. Sci.,* **7**, 1295 (2017).
10. R.K. Brow, *J. Non-Cryst. Solids*, 263-264, **1** (2000).
11. A.A. Setlur, A.M. Srivastava, *Opt. Mater.,* **29**, 410 (2006).
12. Y. Hizhnyi, S.G. Nedilko, V. Chornii et al., *Solid State Phenom*., **200**, 114 (2013).

13. Y.A. Hizhnyi, S.G. Nedilko, V.P. Chornii et al., *J. Alloys Compd.* **614**, 420 (2014).
14. J. Han, L. Li, M. Peng et al., *Chem. Mater.,* **29**, 8412 (2017).
15. Y. Hizhnyi, V. Borysyuk, V. Chornii et al., *J. Alloys Compd*., **867**, 159148 (2021).
16. C.L. Ranganatha, H.S. Lokesha, K.R. Nagabhushana, B.S. Palakshamurthy, *J. Alloys Compd*., **962**, 171061 (2023).
17. K.V. Terebilenko, I.V. Zatovsky, N.S. Slobodyanik et al., *J. Solid State Chem.,* **180**, 3351 (2007).
18. I. Milisavljevic, M.J. Pitcher, J. Li et al., *Int. Mater. Rev.,* **68**, 648 (2023).
19. T. Komatsu, T. Honma, *Int. J. Appl. Glass Sci.,* **4**, 125 (2013).
20. X. Liu, J. Zhou, S. Zhou et al., *Prog. Mater. Sci*., **97**, 38 (2018).
21. Y. Zhang, X. Li, Z. Lai et al., *J. Phys. Chem. C*, **123**, 10021 (2019).
22. T. Honma, K. Maeda, S. Nakane, K. Shinozaki, *J. Ceram. Soc. Jpn.,* **130**, 545 (2022).
23. A. Shearer, M. Montazerian, B. Deng et al., Int. *J. Ceram. Eng. Sci.,* **6**, e10200 (2024).
24. M. Shwetha, B. Eraiah, *IOP Conf. Ser. Mater. Sci. Eng.,* **310**, 012033 (2018).
25. P. Kubelka, *J. Opt. Soc. Am*., **38**, 448 (1948).
26. J. Tauc, R. Grigorovici, A. Vancu, *Phys. Status Solidi B*., **15**, 627 (1966).
27. S. Golbs, F.M. Schappacher, R. Pöttgen et al., *Z. Anorg. Allg. Chem*., **639**, 2139 (2013).
28. A. Mesbah, N. Clavier, E. Elkaim et al., *J. Solid State Chem*., **249**, 221 (2017).
29. R.M. Macfarlane, R.M. Shelby, *J. Lumin*., **36**, 179 (1987).
30. T. Gavrilović, J. Periša, J. Papan et al., *J. Lumin.*, **195**, 420 (2018).
31. C.S. McCamy, *Color Res. Appl.,* **17**, 142 (1992).
32. A.U. Trápala-Ramírez, J.L.N. Gálvez-Sandoval, A. Lira et al., *J. Lumin.*, **215**, 116621 (2019).